# Folding of Influenza Hemagglutinin in the Endoplasmic Reticulum

**Ineke Braakman, Helana Hoover-Litty, Krystn R. Wagner, and Ari Helenius**

Department of Cell Biology, Yale University School of Medicine, New Haven, Connecticut 06510-8002

*Abstract.* The folding of influenza hemagglutinin (HA0) in the ER was analyzed in tissue culture cells by following the formation of intrachain disulfides after short (1 min) radioactive pulses. While some disulfide bonds were already formed on the nascent chains, the subunits acquired their final disulfide composition and antigenic epitopes posttranslationally. Two posttranslational folding intermediates were identified. In CHO cells constitutively expressing HA0, mature HA0 subunits were formed with a half time of 3 min and their folding reached completion at 22 min. The rate of folding was highly dependent on cell type and expression system, and thus regulated by factors other than the sequence of the protein alone. Exposure of cells to stress conditions increased the level of glucose regulated proteins, including BiP, and decreased the folding rate. The efficiency of folding and subsequent trimerization was not dependent on the rate of translation, nor on temperature between 37 and 15°C; however, the rates of folding and trimerization decreased with decreasing temperature. Whereas the rate of folding was independent of expression level, trimerization was accelerated at higher levels of expression.

In mammalian cells, protein folding occurs in three distinct environments: the cytosol, the mitochondria, and the ER. The prevailing conditions in each of these compartments are quite different, and therefore the folding processes display unique properties. For several secretory proteins, it has been shown that folding begins cotranslationally from the $NH_2$-terminus and proceeds towards the COOH-terminus as the polypeptides enter the ER (Bergman and Kuehl, 1979; Jaenicke, 1987). The final outcome is significantly affected by covalent cotranslational modifications such as N-linked glycosylation or the removal of $NH_2$-terminal signal sequences, and by protein disulfide isomerase–catalyzed formation of disulfide bonds (Freedman et al., 1984; Rose and Doms, 1988; Randall and Hardy, 1989). In many cases, the involvement of other folding enzymes, such as proline isomerase, and chaperonins such as binding protein (BiP/GRP78)[1] is likely to be important (Freedman, 1989; Pelham, 1989; Rothman, 1989). The ionic conditions and redox potential in the ER lumen, which are quite distinct from those in the cytosol, may also play an important role. The cell biological aspects of protein folding, however, are poorly understood.

In this paper, we have analyzed the folding of influenza hemagglutinin. The hemagglutinin is a type I transmembrane glycoprotein (84 kD, 549 amino acids) with multiple folding domains (Wilson et al., 1981; Wiley and Skehel, 1987). It is exceptionally well characterized in terms of structure, function, and intracellular transport. In infected or transfected cells, the ectodomain (513 amino acids) is cotranslationally translocated into the ER. Signal peptide cleavage and N-linked glycosylation on five to seven sites occur cotranslationally. When expressed at a high level, the protein forms homotrimers with a half-time of 8 min after synthesis (Copeland et al., 1986; Gething et al., 1986). The trimers are selectively transported to the cell surface via the Golgi complex.

The crystal structure of the ectodomain of the proteolytically activated trimers reveals a 135 Å long trimeric spike protein in which each subunit has two major domains: a globular $NH_2$-terminal top domain and a COOH-terminal domain which forms the stem of the spike protein. The stem region contains the fusion peptides known to be involved in the membrane fusion activity of the protein (Wilson et al., 1981; Wiley and Skehel, 1987). Each HA0 subunit is stabilized by six highly conserved intrachain disulfides.

By following the formation of intrachain disulfides as well as changes in antigenic epitopes, we have determined the rate with which HA0 folds in several cell types, using different expression systems. We analyzed the effects of temperature, translation rate, and stress treatment, and we investigated the relationship between folding, and trimerization and transport. We established that HA0 begins to fold as a nascent chain and continues to fold for several minutes after translation. Unlike trimerization and transport, folding was independent of the level of HA0 expression. Both the rate and efficiency were, however, very different in various cell types and thus significantly affected by cellular factors.

1. *Abbreviations used in this paper*: BiP, binding protein; HA0, influenza hemagglutinin; IT1 and 2, intermediate 1 and 2; NT, native HA0.

## Materials and Methods

### Cell Lines, Recombinant Virus Vectors, and Viruses

CV-1 monkey kidney cells were grown in DME, as previously described (Doxsey et al., 1985), and HeLa cells were grown in minimal essential medium with 10% FCS. CHO cells were grown in alpha minimal essential medium with 8% FCS. A CHO cell line that expresses HA0 constitutively (CHOwtm64s) was developed by Dr. D. Wiley. The transformed cells were grown in alpha minimal essential medium supplemented with 10% FCS, 8 μM methotrexate, and 0.57 mg active G418/ml. The murine 3T3 fibroblast cell line that expresses Japan HA0 constitutively was described by Doxsey et al. (1985).

To express wild-type HA0 from X31 or Japan influenza virus, we used SV40 late replacement vectors containing cDNAs coding for these proteins: pSVEXHA (Doyle et al., 1986) and pSVEHA3 (Gething and Sambrook, 1981), respectively.

Both the X31 (derived from A/Aichi/1986/H3N2) and the Japan strain (A/Japan/305/57/H2N2) of influenza virus were propagated in embryonic eggs as described (Doms et al., 1985). Infectious allantoic fluids were used to infect cells; for high expression levels, the cells were used 5–6 h after infection, whereas for low expression (sevenfold lower), the experiment was started 2 h after infection.

### Antibodies

The polyclonal anti-X31 and anti-Japan virus rabbit sera and the mAb N2 have been previously characterized (Doms et al., 1985; Copeland et al., 1986). The rabbit antisera immunoprecipitate the viral nucleoprotein (56 kD), matrix protein (28 kD), as well as hemagglutinin-folding intermediates, monomers, and trimers. They also immunoprecipitate acid- or SDS-treated and misfolded forms of this protein. The mAb N2 is specific for trimeric X31 HA0. The mAb recognizing BiP (Bole et al., 1986) was a gift of Dr. David Bole (Howard Hughes Medical Institute, Ann Arbor, MI).

To obtain the folding-specific mAbs, F1 and F2, female BALB/c mice were primed with 50 μg of isolated and purified HA2. The antigen was prepared by sequentially treating purified X31 virus with a pH 5.0 buffer, 150 μg/ml TPCK-treated trypsin, and 20 mM DTT. HA2 was then isolated from the protein mixture by phase separation into Triton X-114 as described by Bordier (Bordier, 1981). Detergent was removed on an Extracti-Gel column and the purity and yield of HA2 were checked by SDS-PAGE (Laemmli, 1970). The antigen was mixed with an equal volume of Alu Gel S and injected into the peritoneal cavity of the mouse. An identical boost was given 4 wk later, and after 6 wk, 50 μg was injected into the tail vein. 3 d after the final boost, the spleen was removed from the mouse and the cells were fused with SP2/0 myeloma cells. 10 d after fusion, hybridoma supernatants were collected and screened by ELISA on the purified antigen. Antibody secreting cells were recloned twice in 24-well plates, each time screened by ELISA and by immunoprecipitation of HA0-folding intermediates. F1 is specific for the HA0-folding intermediate IT1 and F2 recognizes the folding intermediate IT2 and the completely folded and disulfide-linked monomeric HA0 (NT, native HA0).

### Metabolic Labeling

Subconfluent cells expressing HA0 were washed twice with PBS and preincubated in methionine- and cysteine-free medium with bicarbonate for 15 min at 37°C. The monolayer was pulse labeled with 40–50 μCi each of [$^{35}$S]cysteine and tran[$^{35}$S]label per 60-mm dish in 400 μl of methionine- and cysteine-free medium with 10 mM Hepes for 1 min unless indicated otherwise. The pulse was ended by adding prewarmed medium with 5 mM each of unlabeled methionine and cysteine. Cycloheximide was included in the chase medium (500 μM) to block completion of nascent chains, except where otherwise indicated. After various chase times the cells were transferred to ice and washed twice with ice-cold PBS, containing 20 mM *N*-ethylmaleimide to prevent the formation of additional disulfide bonds in the protein. The cells were lysed in 2 × 300 μl of ice-cold lysis buffer (0.5% Triton X-100 in MNT [20 mM MES, 100 mM NaCl, 30 mM Tris-HCl, pH 7.5] containing 20 mM *N*-ethylmaleimide, 1 mM EDTA, 1 mM PMSF, and 10 μg/ml each of chymostatin, leupeptin, antipain, and pepstatin).

Lysates were adjusted to the same volume with lysis buffer; the nuclei were pelleted by centrifuging for 5 min at 12,000 *g*. Supernatants were used immediately for immunoprecipitation or velocity gradient centrifugation. Monomers and trimers of HA0 were separated by velocity gradient centrifugation as described by Copeland et al. (1986).

In the temperature dependence studies, HA0-expressing CHO cells were pulse labeled at 37°C for 1 min and then chased at temperatures ranging between 37 and 15°C. The desired chase temperature was rapidly obtained by placing the dishes in a thermostated water bath, and by adding an excess of preincubated chase medium at the appropriate temperature.

Stress treatment of the cells involved 24-h incubation with glucose-free medium (glucose starvation) or 60-min incubation at 43°C (heat shock). The cells were allowed to recover for 2 h in normal medium before the experiment.

To decrease the translation rate of HA0, CHOwtm64s cells were preincubated, pulsed, and chased in media containing 10 μM cycloheximide.

### Immunoprecipitation of HA0 and TCA Precipitation

100 to 300 μl of lysate were used per immunoprecipitation. Goat anti-mouse IgG (5 μl per sample) was incubated for 1 h at 4°C with prewashed, fixed *Staphylococcus aureus* (60 μl of a 10% suspension per sample). The primary mAbs were added (100 μl of tissue culture supernatant containing F1 or F2, 5 μl of purified N2), and incubation was continued for 1 h. Polyclonal antibodies (10 μl of the anti-X31 and 5 μl of the anti-Japan antibody) were incubated directly with *S. aureus* cells for 1 h. The complexes were washed with 0.5% Triton X-100 in PBS and incubated with cell lysates at 4°C for 1 h on an Eppendorf shaker (Brinkmann Instruments Inc., Westbury, NY). The *S. aureus* complexes with the polyclonal antibodies and N2 were washed twice with 1 ml wash buffer (0.05% Triton X-100, 0.1% SDS, 0.3 M NaCl, 10 mM Tris-HCl, pH 8.6) at room temperature; the F1 and F2 complexes were washed with 0.5% Triton X-100 in MNT (20 mM MES, 100 mM Nacl, 30 mM Tris-HCl, pH 7.5). The washed pellets were resuspended in 20 μl 10 mM Tris-HCl, pH 6.8 and sample buffer was added to a final concentration of 200 mM Tris-HCl pH 6.8, 3% SDS, 10% glycerol, 0.004% Bromophenol blue, and 1 mM EDTA.

To determine the amount of radiolabeled protein, 10 μl lysate was mixed with TCA (final concentration: 10% TCA, 0.1% BSA, 1 mM methionine). The precipitate was then boiled in 5% TCA (10 min) to release labeled tRNA from the proteins. After washing with 5% TCA at room temperature and with 100% ethanol, the radioactivity in the pellet was counted in a liquid scintillation counter.

### Endoglycosidase H Digestion

After washing the immunoprecipitates, the final pellet was resuspended in 100 mM sodium acetate, pH 5.5, containing 0.2% SDS and heated to 95°C for 5 min. An equal volume of 100 mM sodium acetate, pH 5.5, was added and one half of each sample was incubated for 16 h at 37°C with 0.5 U of endoglycosidase H. The other half was incubated without endoglycosidase H. Sample buffer with 20 mM DTT (final concentration) was added and samples were analyzed by SDS-PAGE.

### SDS-PAGE, Fluorography, and Quantitation

Samples were heated to 95°C for 5 min, after which they were divided in two. One half received 20 mM DTT and was reheated to 95°C for 5 min. *S. aureus* was removed from all samples by spinning for 5 min at 12,000 *g* and cooled aliquots of the supernatants were loaded in the wells of a 7.5% SDS-polyacrylamide gel for electrophoresis according to Laemmli (1970). When reduced and nonreduced samples were loaded side by side, all samples received 100 mM *N*-ethylmaleimide after cooling. Gels were stained, neutralized, and impregnated with salicylic acid for fluorography with XAR-5 film (Eastman Kodak Co., Rochester, NY). Bands were quantitated by densitometry with a digital gel scanner (Visage 2000). Only gel exposures within the linear range of the film and the scanner response were measured. For photography, longer exposures were usually used.

### Materials

Tissue culture media and G418 sulfate were obtained from Gibco Laboratories (Grand Island, NY). L[$^{35}$S]cysteine (>800 Ci/mmole) and tran[$^{35}$S]label (>1,000 Ci/mmole) were from ICN Biomedicals Inc. (Irvine, CA). Protease inhibitors and methotrexate were purchased from Sigma Chemical Co. (St. Louis, MO) and fixed and killed *S. aureus* was from Zymed Laboratories Inc. (South San Francisco, CA). Goat anti-mouse Ig was obtained from Tago Inc. (Burlingame, CA); endoglycosidase H was from Genzyme Biochemicals Ltd. (Kent, England). Extracti-Gel D detergent removing columns were from Pierce (Rockford, IL).

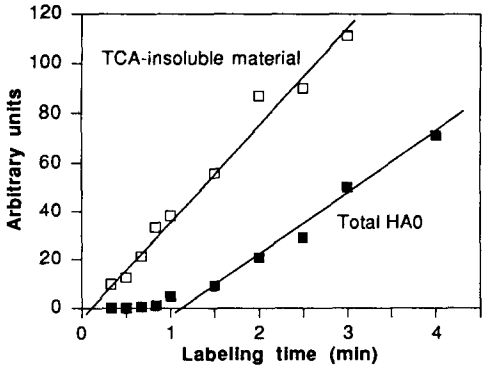


*Figure 1.* Synthesis time of HA0. CHO cells constitutively expressing X31 HA0 were metabolically labeled for indicated times and lysed. TCA-precipitable material was counted to determine incorporation of $^{35}S$ into total protein (□) and immunoprecipitates with a polyclonal antiserum were quantitated for incorporation into HA0 (■). The difference between the intercepts of these lines with the abscissa (10 and 70 s, respectively) equals half the synthesis time of HA0 (2 min) (Horwitz et al., 1969).

## Results

### The Rate of HA0 Translation

Our folding studies concentrated on the time period immediately following HA0 synthesis. It was therefore important to first determine the translation time for HA0. CHO cells permanently expressing HA0 were labeled with a mixture of tran[$^{35}S$]label and [$^{35}S$]cysteine. After different times of continuous labeling, the amount of total labeled protein was determined by TCA precipitation, and the amount of label in full-length HA0 by immunoprecipitation, SDS-PAGE, and scanning densitometry (Fig. 1). Extrapolation of the linear part of the incorporation curves to the abscissa yielded a lag time of 10 s for incorporation of radioactive amino acids into total protein, and a lag time of 70 s for labeling of mature HA0. We concluded that the effective pulse time was 50 s, and that the average synthesis time for HA0 was 120 s, i.e., twice the difference between the observed lag times (for details see Horwitz et al., 1969). This corresponds to a rate of 4.5 amino acids per second.

In subsequent folding experiments, we routinely used a 1 min radioactive pulse. This allowed us to study the events during the first minutes after completed synthesis and it gave sufficient incorporation of radioactivity for accurate quantitation of HA0. The necessity to keep the pulses short introduced a technical problem, which is illustrated in Fig. 2, *a* and *b* and in the quantitative densitometric data in Fig. 2 *d*. The amount of radioactivity in the HA0 band increased dramatically during the first few minutes of chase. This increase suggested that the pulse may have been "leaky," that a large fraction of newly synthesized proteins may be degraded or that the protein may be invisible to the antibody immediately after synthesis.

Additional experiments showed that these were not the reasons for the increase. TCA precipitation of total labeled protein showed that the pulse was very tight: incorporation of [$^{35}S$]methionine and [$^{35}S$]cysteine did not continue after addition of the chase medium (Fig. 2 *d*). Moreover, when a high concentration of cycloheximide (500 μM) was added to the chase medium to block chain elongation immediately after the pulse, the initial increase in labeled full-length HA0 was reduced to ~10% of that observed in the absence of cycloheximide (Fig. 2, *b*, *c*, and *d*). The labeled HA0 remained at a level only slightly higher than observed at the end of the 1-min pulse (at a level of 20–25% of the maximal amount reached after ~5 min of chase without cycloheximide). The cycloheximide was apparently able to rapidly enter the cell and inhibit further chain elongation.

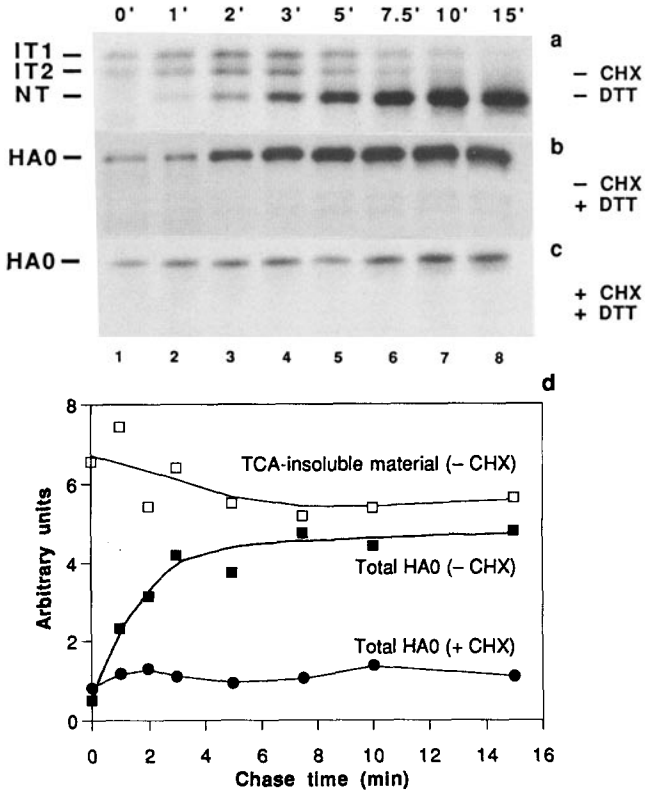


*Figure 2.* The increase in $^{35}S$-labeled full-length HA0 during the chase is because of completion of labeled nascent chains. 5 h after infection with X31 influenza virus, CV-1 cells were pulsed for 1 min. They were chased for indicated time periods without cycloheximide as described in Materials and Methods (*a* and *b*). CHO cells constitutively expressing X31 HA0 were pulse labeled for 1 min and chased for 0–15 min with (*c* and *d*) or without cycloheximide (500 μM; *d*). Reduced (*b* and *c*) or nonreduced (*a*) immunoprecipitates of the lysates were analyzed by 7.5% SDS-PAGE. Trimming of carbohydrates is seen in lanes 6–8. (*d*) Quantitation of gels by scanning densitometry and of TCA-precipitates by liquid scintillation counting.

These results showed that the increase in labeled HA0 in the absence of cycloheximide was caused by completion of nascent HA0 chains that had been labeled but not terminated during the pulse. Extensive degradation of early folding intermediates was not occurring in the cells or in the lysates and the antibodies were evidently able to precipitate virtually all the full-length HA0 in the lysate, regardless of its age. The labeled nascent chains were clearly seen in the immunoprecipitates when the films were exposed somewhat longer. Fig. 3 shows such fluorographs from infected HeLa cells. A smear of nascent chains is visible below the full-length HA0. When cycloheximide was not present during the pulse, the smear rapidly disappeared as the chains were completed and

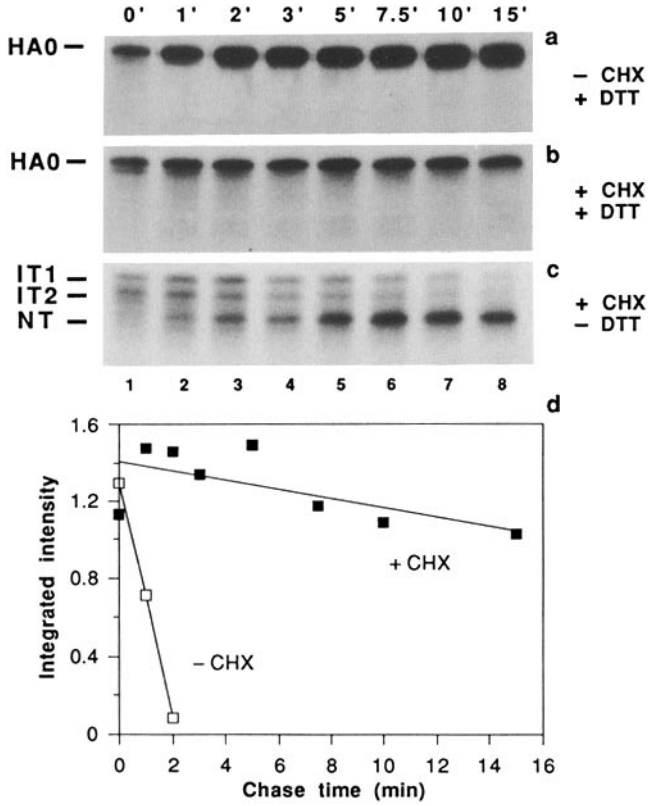


*Figure 3.* Labeled nascent chains are not finished in the presence of cycloheximide. HeLa cells were infected with X31 Influenza virus. 6 h after infection, the cells were pulse labeled for 1 min and chased for 0 to 15 min with (*b* and *c*) or without (*a*) 500 μM cycloheximide. Reduced (*a* and *b*) or nonreduced (*c*) immunoprecipitates of the lysates were analyzed by 7.5% SDS-PAGE. (*d*) Quantitation of gels by scanning densitometry. Nascent chains are visible as a grey smear below the HA0 band, which disappears after 1-min chase in the absence of cycloheximide (*a* and *d*). In the presence of cycloheximide, the nascent chains persist throughout the chase periods (*b*, *c*, and *d*).

the NT band grew stronger (Fig. 3 *a*). In contrast, when cycloheximide was present in the chase medium, the smear persisted throughout the chase period (Fig. 3, *b* and *c*). Fig. 3 *d* shows the quantitation of the results at different times of chase.

A known average synthesis time of a protein allows calculation of the fraction ($f_o$) of incorporated radioactivity that is in the finished protein at the end of the pulse (see Appendix for details). Using the equation for an effective pulse time of 50 s and a synthesis time of 120 s as measured for HA0 we expected to find 21% of HA0-incorporated label in the full-length protein. The 18% we observed after a 1-min pulse (Fig. 2 *d*) was very close to the calculated value, especially when considering the scatter in the densitometric data. The noise in the quantitative data in Fig. 2 *d* and in subsequent experiments was caused by variability in cell number per dish, in sample handling, and in the automatic background reduction during densitometry, all virtually unavoidable given the number of steps involved.

When pulse time and $f_o$ are known the equations can also be used to obtain a rough estimate of the synthesis time. It is worth noting that the synthesis times obtained—whether experimentally determined as in Fig. 1 or calculated with the equations in the Appendix—are average values. The actual synthesis times seem to be variable between individual cells and/or between polysomes. If all HA0 molecules had been synthesized at the same rate, the labeled nascent chains should all have been finished within 2 min of chase in the absence of cycloheximide. That it took about 5 min to reach the maximum level (Fig. 2 *d*) suggests heterogeneity in translation rates.

### *IT1 and IT2 Are Folding Intermediates*

We monitored the formation of intrachain disulfides in the pulse-labeled hemagglutinin, taking advantage of differences in electrophoretic mobility between native HA0 and forms of HA0 with incomplete disulfide bonds (Selimova et al., 1982). To prevent further folding and disulfide bond formation after the end of the chase, the cells were flooded with an ice-cold stop buffer containing 20 mM *N*-ethylmaleimide or 20 mM iodoacetamide, to alkylate remaining free sulfhydryl groups (Creighton, 1978). Lysates were made in a buffer containing nonionic detergent, alkylating agent, and several protease inhibitors. The HA0 was immunoprecipitated from the lysate with a polyclonal anti-HA antibody that recognizes all conformational forms of HA0 (Doms et al., 1985; Copeland et al., 1986; Hurtley et al., 1989). The precipitates were subjected to SDS-PAGE with and without prior reduction with DTT.

After reduction, the HA0 in all the samples migrated as a single band (Figs. 2, *b* and *c*, and 3, *a* and *b*). After a 7.5-min chase in CHO cells this band underwent a slight increase in electrophoretic mobility because of carbohydrate trimming (Fig. 2 *c*, lane *6*) (Copeland et al., 1986) and a subsequent decrease because of terminal glycosylation (Matlin and Simons, 1983; Copeland et al., 1986). When the corresponding samples were not reduced, up to three separate HA0 bands could be distinguished (Figs. 2 *a*, and 3 *c*). The three bands all ran faster on the gel than fully reduced HA0 (Fig. 4, lanes *1* and *2*). The most rapidly migrating band corresponded to the native fully oxidized HA0 (designated NT). The two other bands (designated intermediate 1 [IT1] and intermediate 2 [IT2]) migrated between NT and the fully reduced HA0 (Fig. 4, lanes *1* and *2*). IT1 and IT2 disappeared during the chase while NT became stronger.

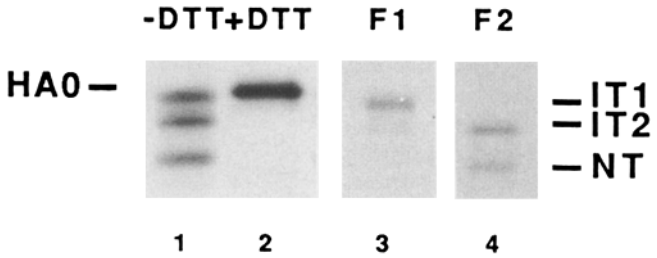


*Figure 4.* Electrophoretic mobility and conformation of IT1, IT2, and NT. Reduced (lane *4*) and nonreduced (lane *3*) immunoprecipitates from the 2-min chase lysate of Fig. 2 *a* and *b* were run side by side. The reduced HA0 has a lower mobility than any of the forms of nonreduced HA0. Immunoprecipitation of this lysate with the conformation-specific mAbs F1 and F2 shows that F1 recognizes IT1 (lane *1*), whereas F2 recognizes IT2 and native HA0 (lane *2*).

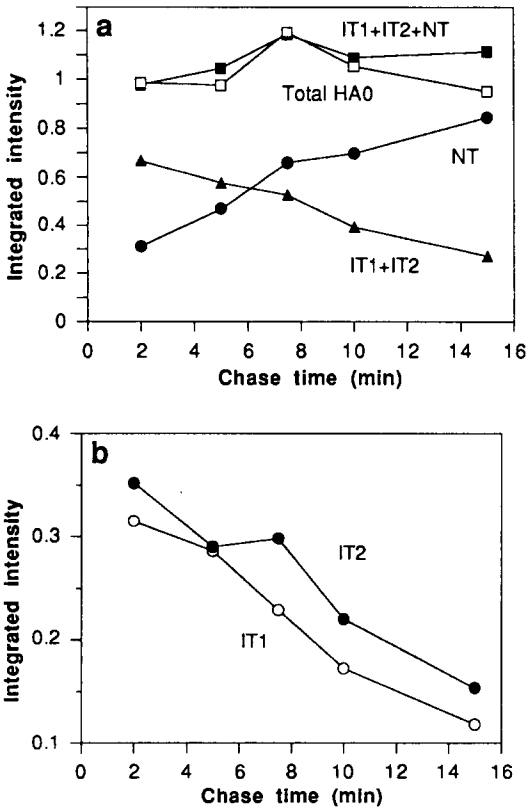


*Figure 5.* Precursor–product relationship of IT1 and IT2 with NT. CHO cells constitutively expressing X31 HA0 were pulse labeled for 1 min at 37°C and chased for up to 15 min with 500 μM cycloheximide at 30°C. Reduced or nonreduced immunoprecipitates of the lysates were analyzed by 7.5% SDS-PAGE. Bands were quantitated by scanning densitometry. (*a*) NT increases while IT1 + IT2 decreases; the sum of the nonreduced bands is equal to the reduced full-length HA0 and stays constant during the chase. (*b*) IT1 and IT2 disappear with very similar rates.

No HA0 band was ever seen at the position of the fully reduced HA0 when cell lysates were analyzed (Fig. 4). This indicated that a fully reduced, full-length HA0 did not exist as an intermediate in the cell. Hence, one or more intramolecular disulfide bonds were already formed on the nascent HA0 chain. In other words, folding and disulfide bond formation began cotranslationally. This has been shown previously for soluble secretory proteins (Bergman and Kuehl, 1979; Peters et al., 1982).

The electrophoretic mobility of the two transiently expressed HA0 forms, IT1 and IT2, showed that they represented full-length molecules with incomplete or aberrant intrachain disulfide bonds. When reduced, they migrated with fully reduced HA0 (Fig. 4, lane *2*), when nonreduced they migrated between the nonreduced, native HA0 (NT) and the fully reduced mature HA0 (Fig. 4, lane *1*). In addition to being different in their disulfide bond composition, the intermediates were clearly different in conformation, as judged by their antigenic properties. When preparing conformation-specific mAbs against isolated HA2 subunits, we found one mAb (called F1) that immunoprecipitated only IT1 (Fig. 4, lane *3*), and another (called F2) that precipitated IT2 and NT, but not IT1 (Fig. 4, lane *4*).

The observation that the amount of labeled IT1 and IT2 during the chase decreased as the label in NT increased, suggested that they were folding intermediates of NT. Using cyclohexmide to suppress the increase in HA0 label during the chase, we could address this apparent precursor–product relationship quantitatively. Fluorographs from a pulse–chase experiment in HA0-expressing CHO cells were scanned, and the integrated optical intensities of the three bands determined. We excluded the data from the first 2 min of chase, since some increase in labeled HA0 still occurred there, probably because of the time it takes for the cycloheximide to reach its site of action. It is clear from Fig. 5 *a* that, in the time period analyzed, the total amount of labeled HA0 was essentially constant, and that the sum of the intensities of the IT1, IT2, and NT bands was constant and equal to the intensity of reduced full-length HA0. Moreover, NT doubled in intensity while IT1 and IT2 decreased. The results clearly show that IT1 and IT2 must be precursors for NT. When plotted separately (Fig. 5 *b*), it could be seen that the optical intensities of the IT1 and IT2 bands decreased in parallel. Given the noise in the data, however, it was impossible to determine whether they were each others precursors or independent precursors of NT.

The half time of folding was defined as the time at which 50% of the labeled HA0 reached the mature form NT. In permanently expressing CHO cells the half time of folding was 3.2 min at 37°C and at 30°C it was around 6 min. The values were highly reproducible from one experiment to the next. In some cases, the half time was determined in the absence of cycloheximide from the time at which IT1 plus IT2 were equal to NT. While less accurate, this value was generally similar to that obtained with cycloheximide in the chase medium. The inclusion of cycloheximide did not seem to have any adverse effects on folding and trimerization (see below).

### *Folding Rates Differ between Cells*

Next, the folding process was compared in different cell lines and expression systems, using hemagglutinins from different influenza virus strains. Four different cell types were tested: NIH 3T3 cells, HeLa cells, CHO K1 cells, and CV-1 cells. HA0 was expressed using either influenza infection (in all four cell types), transfection using an SV-40 recombinant virus (in CV-1 cells), or by permanent expression (in CHO and 3T3 cells). HA0s from the X31 (derived from A/Aichi/1986/H3N2) and the Japan (A/Japan/305/57/H2N2) strains of influenza A were tested. While the amino acid sequences of the two HA0 molecules show only 42% similarity, the number and location of the cysteine residues in the ectodomain is fully conserved. The half time of folding was determined as described above. We also defined the end time, the time needed for folding intermediates to disappear, because we observed that half time and end time were not necessarily coupled. Measurements of both parameters were found to be very reproducible. We used the half time as a measure of the rate of folding, and end time as a measure of the efficiency of folding. We defined the efficiency of folding as the percentage of HA0 that finally reaches the folded state NT. Folding reached >95% efficiency in all tested systems except in HeLa cells: a small fraction of HA0 failed to fold completely.

The same two folding intermediates, IT1 and IT2, were always observed for X31 HA0, regardless of cell type and ex-

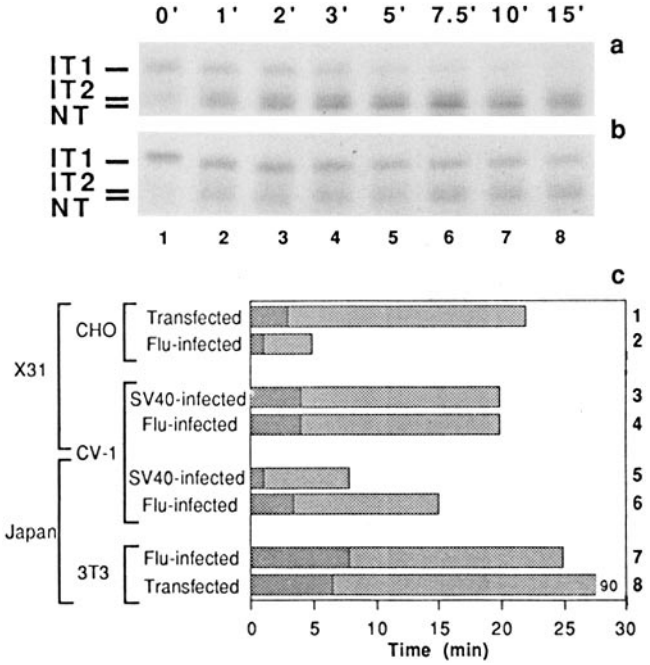


*Figure 6.* Cell type and expression system affect folding of HA0. (*a*) Example of fast folding. Japan HA0 expressed in CV-1 cells by recombinant SV-40 infection. (*b*) Example of slow folding. Japan HA0 constitutively expressed in 3T3 cells. IT2 and native HA0 migrate close together and are more difficult to discern than for X31 HA0. (*c*) The folding assay was carried out as described, for X31 and Japan HA0, in different cell lines, using different expression systems. Dark areas in the bars denote half times, total length of the bars denotes end time of folding.

pression system (although they were not always present in equal ratios). In Japan HA0, the counterpart for the IT2 intermediate was sometimes difficult to discern because it migrated very close to NT (Fig. 6 *b*). No other consistent differences were observed between the two HA0 subtypes, suggesting that they fold in a similar manner.

A striking difference in the folding kinetics was observed between the various cells and expression systems. As shown in Fig. 6 *c*, the half times varied between 1 and 8 min and the end times varied between 5 and 90 min. An example of such differences in folding of Japan HA0 is illustrated in Fig. 6, *a* and *b*. The differences displayed in Fig. 6 *c* were not because of differences in synthesis rates, as the increase in labeled HA0 during the first few minutes of chase (in the absence of cycloheximide) was the same in each case (Fig. 2 *d*). Nor were they caused by differences in the primary sequence of the proteins synthesized in the various expression systems, as the cloned X31 as well as the cloned Japan HA0 genes were identical. We concluded that the differences were cell-type dependent, and that the kinetics of HA0 folding were determined not only by the primary structure of the protein but also by the cellular context. Furthermore, the cellular factors appeared to be sensitive to the conditions used for expression and culture.

### *Folding Rates Are Affected by Virus Infection and Stress*

Folding of HA0 was generally faster and/or more efficient in cells infected with influenza or SV40 than in cells permanently expressing the proteins (Fig. 6 *c*). To determine whether the folding of both the constitutively expressed HA0 and the HA0 of the infecting virus was accelerated, we infected X31-HA0–expressing CHO cells with Japan influenza, and Japan-HA0–expressing 3T3 cells with X31 influenza. In both cases the folding of the constitutively expressed hemagglutinins was accelerated (Fig. 7 *a*; lanes *1*, *2*, *4*, and *5*), but not to the same extent as the folding of the infecting HA0 (lane *3*). Hence, the stimulating influence of infection on folding was preferentially seen for the hemagglutinin of the infecting virus. The basis for this surprising effect remains unclear.

The slower folding process observed in the stably expressing cells could also be caused by differences between the transfected and the parental cell lines (as a result of transfection, selection, or differentiation). To test this possibility, we followed the folding of an infected HA0 in both the stably expressing cells and in their parent cell lines (3T3 and CHO). Unexpectedly, both transfected cell lines were more efficient and faster in folding HA0 than were their parent cell lines (Fig. 7 *b*). This only magnified the differences in folding rates between infected and stably expressed HA0s (Figs. 6 *c* and 7 *a*).

Since cellular stress proteins have been implicated in the folding process, and since such proteins are often induced by viral infection (Garry et al., 1983), we submitted the X31-expressing CHO cells to heat shock and glucose starvation, conditions that are known to increase the expression of heat

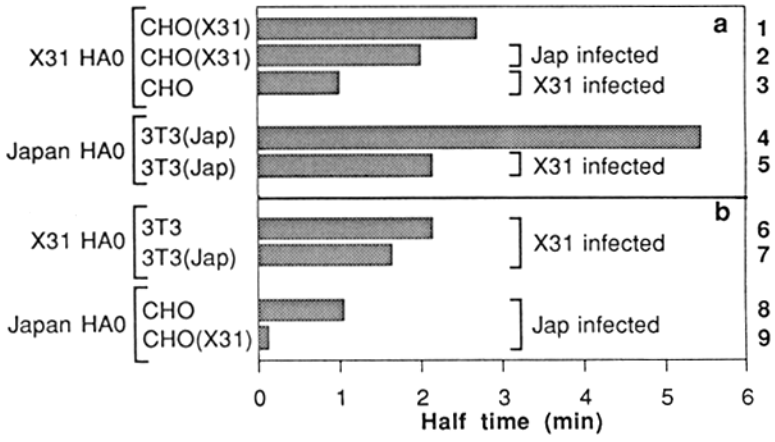


*Figure 7.* Viral infection accelerates folding of HA0. (*a*) Cells constitutively expressing HA0 (described as CHO[X31] or 3T3[Jap]) were used in the folding assay after infection with an Influenza strain carrying an antigenically distinct HA0. Folding of only the endogenous HA0 was followed. (*b*) Folding of the infecting HA0 was quantitated in the constitutively expressing cells and compared to untransfected CHO and 3T3 cells.

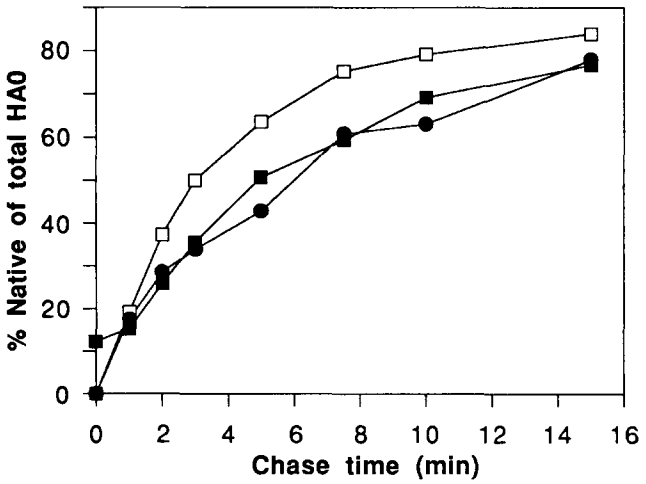


*Figure 8.* Effect of stress on HA0 folding. CHO cells stably expressing X31 HA0 were subjected to overnight glucose starvation (■) or to 60-min heat shock (●) before being used in the folding assay. Cells were allowed to recover for 2 h before the pulse chase started. (□) Untreated cells.

shock proteins and GRPs in the ER. The cells were allowed to recover for 2 h in normal medium, and HA0 folding rates were determined. A significant change was observed: the half time in the stressed cells was 5.2 min whereas it was 3.0 min in cells that had not undergone stress treatment (Fig. 8). Immunoblotting with an antibody to BiP confirmed that the level of BiP (GRP78) had increased more than sixfold after the stress treatments (data not shown). We assume that the other GRPs had also been elevated by the stress treatment.

### *Trimerization Is Concentration Dependent, Folding Is Not*

To determine whether the rate of folding and subsequent trimerization and transport were concentration dependent, we analyzed CHO cells at two different times after influenza X31 infection. 2 h postinfection, the amount of HA0 synthesis was sevenfold lower than it was 6 h postinfection. The half times of folding were found to be identical (Fig. 9). Although folding half times were the same, the efficiency of folding was slightly lower at the higher expression level: the folding intermediates were still present at the 15 min chase time (Fig. 9 *b*).

The rate of trimerization (assayed by immunoprecipitation with a trimer-specific mAb, N2) was considerably faster at 6 h ($t_{½}$ = 8 min) than at 2 h ($t_{½}$ = 19 min). The results indicated that the rate of folding was essentially concentration independent, whereas trimerization was dependent on the level of HA0 expression.

In addition, the acquisition of endoglycosidase H resistance was analyzed to determine whether the kinetics of HA0 transport to the Golgi complex were concentration dependent. Since our previous results have indicated selective transport of trimers from the ER (Copeland et al., 1986; Doms et al., 1987), we expected to find slower transport at the lower expression level as a consequence of the delay in trimerization. The acquisition of endoglycosidase H resistance was, indeed, found to be slower but the difference was smaller than expected. The half time was 19 min at the high expression level and 22 min at the low expression level (Fig. 9). This raised the possibility that monomers were transported to the Golgi complex when the expression levels and

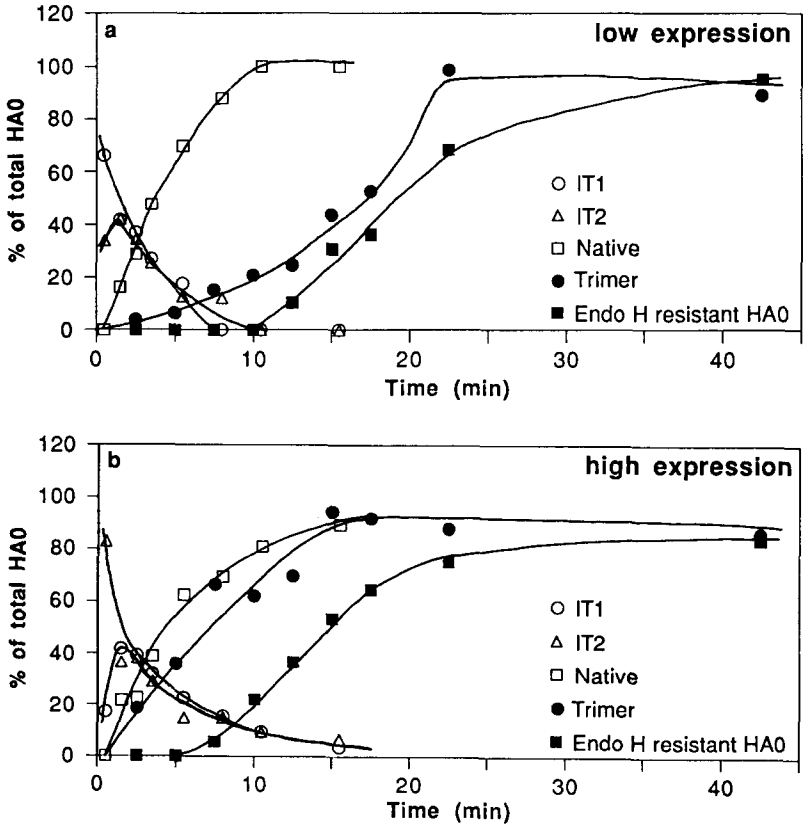


*Figure 9.* Concentration dependence of HA0 folding, trimerization, and transport to the Golgi complex. CV-1 cells were used 2 h (*a*) and 6 h (*b*) after infection with X31 Influenza. Folding rate was determined as described in Materials and Methods, trimers were detected by immunoprecipitation with the trimer-specific antibody N2, and transport to the *medial*-Golgi was assayed by endoglycosidase H digestion of samples immunoprecipitated with a polyclonal anti-HA0 antiserum.

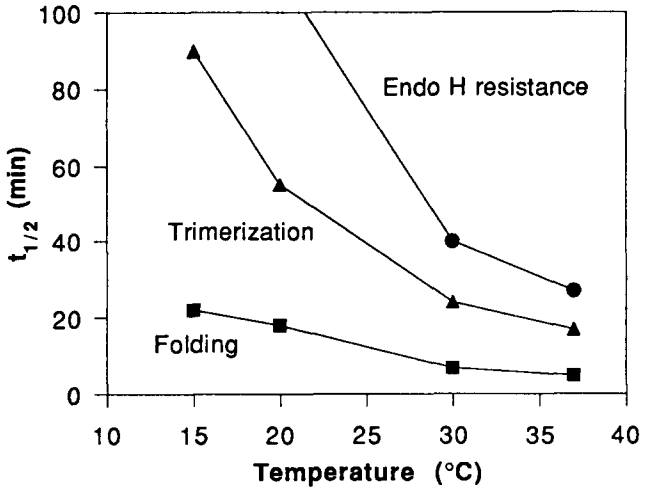


*Figure 10.* Temperature dependence of HA0 folding, trimerization, and transport to the Golgi complex. CHO cells stably expressing X31 HA0 were pulse labeled for 1 min at 37°C and then chased at 37, 30, 20, or 15°C. Assays were done as in Fig. 7.

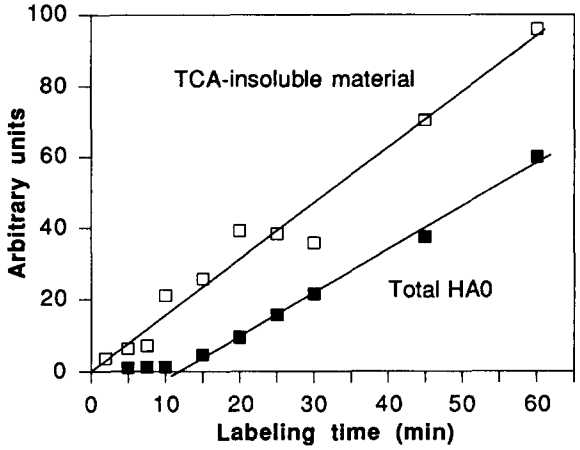


*Figure 11.* Synthesis time of HA0 in the presence of 10 μM cycloheximide. Experimental conditions were as in Fig. 1, except that 10 μM cycloheximide was added to the preincubation medium and the pulse medium.

trimerization rates were low. Analyzing the labeled trimers and monomers at different times of chase using sucrose velocity gradient fractionation, however, gave no indication of monomers in the Golgi complex (not shown). At no time during the chase, whether at low or high levels of HA0 expression, did we detect endoglycosidase H-resistant HA0 in the 4.5S monomer fraction. The results provided support for previous reports from our group and others, that HA0 monomers do not reach the Golgi complex (Copeland et al., 1986; Gething et al., 1986; Doms et al., 1987; Ceriotti and Colman, 1990).

### *Temperature Dependence of Folding, Trimerization, and Transport*

To study the temperature dependence of posttranslational folding, trimerization, and transport, HA0-expressing CHO cells were pulse labeled at 37°C for 1 min, and chased at temperatures between 37 and 15°C. At the onset of the chase, the samples contained a mixture of intermediates IT1 and IT2, but little or no NT (Fig. 2 *a*, lane *1*).

While the efficiency of folding and trimerization remained uniformly high at all temperatures (>95%), the rates decreased with decreasing temperature (Fig. 10). A drop in temperature from 37 to 27°C caused a doubling of the folding time, a 40% increase in the trimerization time and an 80% increase in the transport time. The order of events, folding, trimerization and transport, was preserved throughout the temperature range except at 15°C and below, where folding and trimerization occurred but transport to the Golgi complex was blocked (Saraste and Kuismanen, 1984). At 37°C, both folding intermediates IT1 and IT2 disappeared with similar rates (Figs. 2 *a*, 3 *c*, and *9*). At lower temperatures, however, IT1 disappeared faster than IT2.

### *Folding and Trimerization Are Independent of Translation Rate*

Cycloheximide was used to determine whether a decrease in translation rate would affect HA0 folding and trimerization. While causing virtually complete inhibition of protein synthesis at concentrations above 100 μM, cycloheximide merely slowed down the rate of synthesis when added to cells at lower concentrations. The translation time for HA0 in the presence of 10 μM cycloheximide was determined as in Fig. 1 (Fig. 11). The average synthesis time for HA0 was delayed to ~25 min instead of the 2 min observed in untreated cells. This is in agreement with the increase in full-length labeled HA0 during the chase, seen in Fig. 12 *a* up to lane *10* (30-min chase). The half time for trimerization, determined by immunoprecipitation with the trimer-specific antibody N2, was ~60 min (Fig. 12 *b*).

When folding and trimerization were analyzed in the presence of 10 μM cycloheximide, several observations were made: (*a*) The decrease in translation rate did not affect the efficiency of folding: virtually all of the detectable protein reached the native state. (*b*) The pathway of folding was not affected judging by the presence of the IT1, IT2, as well as the NT form of HA0 at different times of chase (e.g., lane *9*). (*c*) Synthesis was rate limiting, as indicated by the low amounts of intermediates present at any time. (*d*) The efficiency of trimerization was normal, but the rate was slowed down from a normal half time of 8 min after synthesis to a half time of ~30 min after synthesis. This was predictable in view of the concentration dependence of HA0 trimerization as demonstrated above. A decrease in synthesis rate must have led to a decrease in HA0 concentration in the ER at any given time during pulse and chase.

## *Discussion*

The available data on the folding of multidomain proteins in the ER indicate that the translocated portion of a polypeptide begins to fold before the entire polypeptide chain has been synthesized. Such "vectorial folding" has been reported for IgG heavy chains (Bergman and Kuehl, 1979), for BSA (Peters and Davidson, 1982) and for other proteins (for review see Jaenicke, 1987). Our results provide evidence for vectorial folding of HA0, a membrane glycoprotein. We found that the first detectable full-length HA0 already possessed some, but not all, of the intrachain disulfide bonds. Additionally, conformation-dependent antigenic epitopes present in the

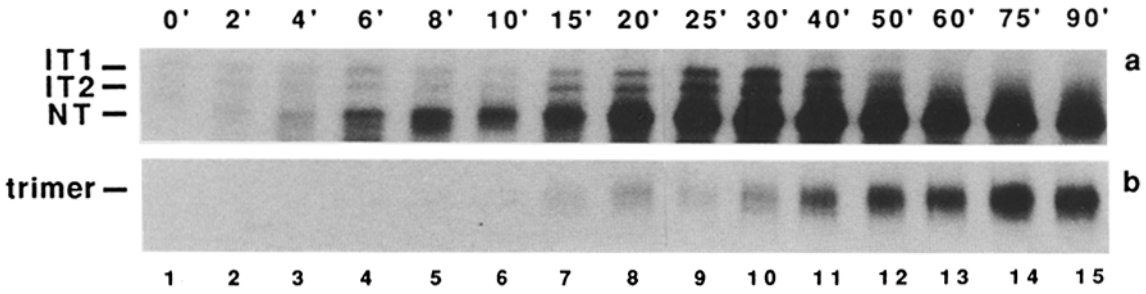


*Figure 12.* Slow translation of HA0 does not affect the folding processes. CHO cell stably expressing X31 HA0 were pulse labeled for 2 min and chased for 0 to 60 min. 10 μM cycloheximide was present throughout, to increase the synthesis time of HA0. (*a*) 7.5% nonreducing SDS-PAGE. Folding intermediates are present only in low amounts compared to native HA0. Folding is complete after ~60 min chase. (*b*) 7.5% reducing SDS-PAGE; immunoprecipitation with trimer-specific antibody. Folded monomers do trimerize, though slowly.

fully folded subunit were also present in some of the nascent chains. Consequently, the folding process occurred cotranslationally as well as posttranslationally. Since we have focused on changes in the full-length HA0, our data primarily concern the posttranslational folding steps.

The rate of translation obviously provides a lower limit for how fast folding of a protein can take place in the living cell. The average translation rate for HA0 at 37°C was ~4.5 amino acids per second, and the average synthesis time was 120 s. This is similar to the rate of biosynthesis of most eukaryotic proteins (Knopf and Lamfrom, 1965; Horwitz et al., 1969; Vuust and Piez, 1972). The radioactive pulse time of 60 s routinely used in our experiments corresponded to ~50 s of effective incorporation time. The shortness of this time relative to the time of synthesis explained why only a fraction of the label incorporated into HA0 was found in the full-length protein at the end of the chase. The rest of the label was in nascent chains, which were completed during the first 5 min of the chase. This phenomenon resulted in an apparent increase in HA0 labeling during the chase, which has previously confounded investigators who used short pulses (Lazarovits et al., 1990). Since the pulse-chase approach is one of the few methods available to analyze folding in vivo, this intrinsic problem must be controlled when studying events that occur cotranslationally or immediately after completed synthesis. We found that one way to do this is to add cycloheximide to the chase medium, and so prevent the completion of nascent chains. Not only does this make the pulse sharper, it also allows the determination of precursor–product relationships for folding intermediates.

Cycloheximide can also be used to slow down translation. We found that a concentration of 10 μM of this reversible elongation inhibitor decreased the synthesis rate of HA0 12-fold. The efficiency of folding, trimerization and transport were not affected. A decreased synthesis rate thus did not adversely affect the final outcome of co- and/or posttranslational HA0 folding. This conclusion was supported by results at different temperatures: we found that while synthesis rates and folding rates decreased with decreasing temperature, the efficiency of folding and trimerization remained high.

The change in electrophoretic mobility of alkylated, nonreduced HA0 upon formation of intrachain disulfides provided a simple assay for folding. It has been extensively used both in vivo and in vitro experiments before (Creighton, 1978). The ectodomain of the mature protein has twelve cysteines, all of which are part of intrachain disulfide bonds. Two of them (14-465 and 52-277) form large loops in the protein, which may explain the large difference in mobility between reduced and nonreduced HA0 (Fig. 4, lanes *3* and *4*). Two folding intermediates (IT1 and IT2) were seen. The missing disulfide crosslinks in these intermediates have not yet been identified, but they may correspond to the two loop-forming disulfides. Differential reactivity with conformation specific monoclonals indicated that IT1, IT2, and the native form were conformationally distinct. In Japan HA0, two folding intermediates were seen as well, but one of them (IT2) had a different electrophoretic mobility than either of the X31 HA0 intermediates.

The posttranslational folding rates for HA0 varied significantly among cell types, indicating that the cellular context affected the rate and efficiency of HA0 folding. When cells permanently expressing HA0 were infected with influenza virus possessing an HA0 that could be distinguished from the constitutively expressed HA0, the infecting virus accelerated folding of the constitutively expressed HA0, although not to the same extent as the folding of its own HA0. Apparently, viral infection caused a general acceleration in HA0 folding. The reason why there was still a difference in rate between the constitutively expressed and the infected HA0s remains unexplained.

We assayed the folding rate in cells containing elevated amounts of stress proteins, induced by heat shock or glucose starvation. This was of interest since these proteins are thought to play a role in folding (Rothman, 1989). In the stressed cells, the folding of HA0 was slower than in control cells. More detailed studies are needed to determine which stress-induced protein(s) or which changes are responsible for this effect. It is noteworthy in this context that HA0 does not bind detectable amounts of BiP during folding (Hurtley et al., 1989). Transient association of BiP with folding intermediates has been described for several other glycoproteins (Bole et al., 1986; Machamer et al., 1989; Ng et al., 1989). It will be of interest to determine whether their folding depends on BiP concentration.

We also determined the effect of expression level on the rates of folding, trimerization, and transport. No difference was found in the half time of folding over a sevenfold range in expression level. The somewhat longer end time for folding at high expression levels suggested, however, that the process may become saturated at very high levels of expression, but this needs to be confirmed. In the same experiments, we observed a clear-cut concentration dependence of trimerization. Trimers formed with a half time of 8 and 19 min at the high and low expression levels, respectively. The

results were confirmed by the experiments in which the translation rate of HA0 was decreased by cycloheximide (Fig. 12 *b*). When the synthesis rate of HA0 was around 10-fold lower than in untreated cells, trimerization of HA0 was much slower than could be accounted for by a slower synthesis. After correction for synthesis time, trimerization was delayed more than 20 min compared to untreated cells. The concentration dependence of trimerization revealed by these experiments was consistent with recent data in Xenopus oocytes transfected with different amounts of HA0 mRNA, where trimerization of HA0 was also clearly concentration dependent (Ceriotti and Colman, 1990), and with our previous observations that trimers assemble from a mixed pool of monomers (Boulay et al., 1988).

From a theoretical point of view, the difference in trimerization rate (2.5-fold over a sevenfold concentration range) was surprisingly small. If trimerization were an ideal second-order reaction, a sevenfold increase in concentration would yield a 49-fold faster trimerization rate and a sevenfold lower half time. The likelihood that trimerization corresponds to two second-order reactions, and that it occurs in a two-dimensional membrane system (Grasberger et al., 1986), would tend to further increase the anticipated difference. A more complete analysis of the concentration dependence of oligomerization in the ER is clearly needed. At present, we suspect that HA0 trimerization is a multi-step reaction, which involves second- as well as zero-order reactions, both of which contribute to the overall kinetics.

Judging from the acquisition of endoglycosidase H resistance, the transport of HA0 to the Golgi apparatus was slower at the lower expression level than it was at the higher expression level ($t_{½}$ of 22 vs. 19 min). This difference was smaller than expected, based on the decreased rate of trimerization. We considered the possibility that HA0 could leave the ER, reach the Golgi complex, and become endoglycosidase H resistant as a monomer. While the exact location of trimerization is still debated (Yewdell et al., 1988; Hurtley and Helenius, 1989; Lazarovits et al., 1990), monomer transport of HA0 into the Golgi complex has not been observed in tissue culture cells (Copeland et al., 1986; Gething et al., 1986; Copeland et al., 1988; Yewdell et al., 1988) or Xenopus oocytes (Ceriotti and Colman, 1990). We addressed this question by velocity gradient centrifugation, and found no endoglycosidase H–resistant HA0 in the 4.5S monomer peak. The fast transport of HA0 at low expression levels must therefore have another explanation. Perhaps it is caused by a difference in the secretory pathway early and late during viral infection, by a saturable transport mechanism, or by the presence of a transport competent HA0 trimerization intermediate, that is not detected by the trimer specific antibodies.

Together with previous work on quality control in the ER (Lodish, 1988; Rose and Doms, 1988; Hurtley et al., 1989; Klausner, 1989), our results provide a partial explanation for why the rates and efficiencies with which proteins are transported from the ER are so different. For soluble and membrane proteins, the half times vary from ~10 min to several hours (Lodish et al., 1983; Fries et al., 1984; Matter and Hauri, 1991). The efficiency of transport also varies widely. Clearly, the most important factors are the rate and efficiency of folding of the individual proteins and, when appropriate, the rate and efficiency of oligomer assembly. The folding rate is determined by the nature of the polypeptide chain and, as documented in this paper, by cellular factors and conditions. As a first approximation, folding rates are independent of expression level. The rate of oligomeric assembly depends on the complexity of the quaternary structure (the number of different subunits, the number of subunits in the complex, the architecture of the complex), and on the concentration of subunits in the ER. Once the oligomers have formed, transport to the Golgi complex takes place. Whether the transport is concentration dependent as suggested by the bulk flow model (Pfeffer and Rothman, 1987), needs to be further investigated. Slow transport of a protein is, according to our view, caused by slow folding, a low expression level, and slow assembly. Inefficient transport is caused by misfolding and incomplete assembly.

It is noteworthy that all the early events we studied displayed asynchronism. While the average time for HA0 biosynthesis was 2 min, our results suggested that some labeled polypeptide chains were still being synthesized as late as 5 min after the pulse. Individual polypeptide chains labeled during a 1-min pulse, took 1–20 min to fold, and 20–30 min to trimerize. The lack of synchronism at each step of the pathway explains why proteins synthesized together in the ER, reach the plasma membrane over a wide time period.

## *Appendix*

If the average synthesis time of a protein is known, one can calculate what fraction of the radioactivity associated with the protein at the end of a pulse will be incorporated into the completed polypeptide chains. Protein synthesis can be depicted as in the figure. It is assumed that initiation occurs continuously (in the figure from left, *N*, to right, *C*) that the elongation rate is constant, that the specific activity of incorporated radioactive label is constant during the effective pulse, and that methionines and cysteines are evenly spaced over the amino acid sequence.

The horizontal lines depict the synthesis of polypeptide chains, starting from the $NH_2$ terminus; the length of the lines ($s$) is the average synthesis time; $p$ is the effective pulse time (i.e., the actual pulse time minus the lag in radioactive incorporation, see Fig. 1); $a$ is a parameter corresponding to the number of nascent chains of the protein at any given point in time. The amount of radioactivity incorporated is represented by shaded surface areas in the figure. At the end of a pulse, the amount of radioactive label present in nascent and completed protein is $a \times p$. The amount in completed proteins is shown in darker grey, the amount in nascent chains in lighter grey.

For calculating the fraction ($f_o$) of incorporated radioactive label in the completely translated protein, two different equations apply, depending on whether the pulse is longer or shorter than the synthesis time.

When $p < s$, $f_o$ is $(b \times p \times 0.5)/(a \times p)$. Since $\tan \beta$ equals $a/s$ equals $b/p$, $f_o$ is $p/2s$. When $p > s$, $f_o$ is $\{(a \times s \times 0.5) + (e \times s)\}/(a \times p)$. Since $\tan \beta$ equals $a/s$ equals $e/(p - s)$, $f_o$ is $\{(a \times s \times 0.5) + a(p - s)\}/a \times p$, being $1 - s/2p$. When $p = s$, both equations apply, and $f_o$ will be 0.5.

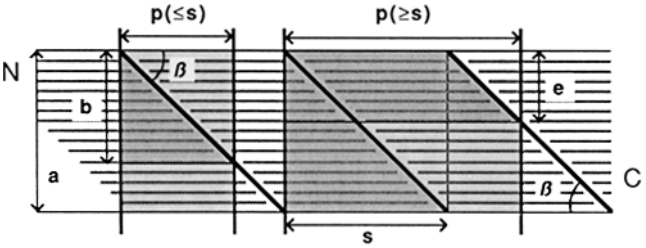

Figure Appendix

We thank Dr. D. C. Wiley for the recombinant CHO cell line, Drs. M.-J. Gething and J. Sambrook for the recombinant viruses, and Dr. D. Bole for the anti-BiP antibody. Martina Ittensohn is gratefully acknowledged for help with the preparation of mAbs, Philippe Male and Henry Tan for photography, and Kelsey Martin for critically reading the manuscript.

This work was supported by grants from the National Institutes of Health to Ari Helenius. Ineke Braakman was supported by post-doctoral fellowships from the James Hudson Brown-Alexander B. Coxe Foundation and from the Human Frontier Science Program Organization.

Received for publication 18 December 1990 and in revised form 17 April 1991.

### *References*

Bergman, L. W., and W. M. Kuehl. 1979. Formation of an intrachain disulfide bond on nascent immunoglobulin light chains. *J. Biol. Chem.* 254:8869–8876.

Bole, D. G., L. M. Hendershot, and J. F. Kearney. 1986. Posttranslational association of immunoglobulin heavy chain binding protein with nascent heavy chains in nonsecreting and secreting hybridomas. *J. Cell Biol.* 102:1558–1566.

Bordier, C. 1981. Phase separation of integral membrane proteins in Triton X-114 solution. *J. Biol. Chem.* 256:1604–1607.

Boulay, F., R. W. Doms, R. G. Webster, and A. Helenius. 1988. Posttranslational oligomerization and cooperative acid activation of mixed influenza hemagglutinin trimers. *J. Cell Biol.* 106:629–639.

Ceriotti, A., and A. Colman. 1990. Trimer formation determines the rate of influenza haemagglutinin transport in the early stages of secretion in *Xenopus* oocytes. *J. Cell Biol.* 111:409–420.

Copeland, C. S., R. W. Doms, E. M. Bolzau, R. G. Webster, and A. Helenius. 1986. Assembly of influenza hemagglutinin trimers and its role in intracellular transport. *J. Cell Biol.* 103:1179–1191.

Copeland, C. S., K.-P. Zimmer, K. R. Wagner, G. A. Healey, I. Mellman, and A. Helenius. 1988. Folding, trimerization and transport are sequential events in the biogenesis of influenza virus hemagglutinin. *Cell.* 53:197–209.

Creighton, T. E. 1978. Experimental studies of protein folding and unfolding. *Prog. Biophys. Molec. Biol.* 33:231–297.

Doms, R. W., A. Helenius, and J. White. 1985. Membrane fusion activity of the influenza virus hemagglutinin. The low pH-induced conformational change. *J. Biol. Chem.* 260:2973–2981.

Doms, R. W., D. S. Keller, A. Helenius, and W. E. Balch. 1987. Role of adenosine triphosphate in regulating the assembly and transport of vesicular stomatitis virus G protein trimers. *J. Cell Biol.* 105:1957–1968.

Doxsey, S. J., J. Sambrook, A. Helenius, and J. White. 1985. An efficient method for introducing macromolecules into living cells. *J. Cell Biol.* 101: 19–27.

Doyle, C., J. Sambrook, and M.-J. Gething. 1986. Analysis of progressive deletions of the transmembrane and cytoplasmic domains of influenza hemagglutinin. *J. Cell Biol.* 103:1193–1204.

Freedman, R. B. 1989. A protein with many functions? *Nature (Lond.).* 337: 407–408.

Freedman, R. B., B. E. Brockway, and N. Lambert. 1984. Protein disulfide isomerase and the formation of native disulfide bonds. *Biochem. Soc. Trans.* 12:929–932.

Fries, E., L. Gustafsson, and P. A. Peterson. 1984. Four secretory proteins synthesized by hepatocytes are transported from the endoplasmic reticulum to the Golgi complex at different rates. *EMBO (Eur. Mol. Biol. Organ.) J.* 3:147–152.

Garry, R. F., E. T. Ulug, and H. R. Bose. 1983. Induction of stress proteins in Sindbis virus- and vesicular stomatitis virus-infected cells. *Virology.* 129:319–332.

Gething, M.-J., and J. Sambrook. 1981. Cell-surface expression of influenza haemagglutinin from a cloned DNA copy of the RNA gene. *Nature (Lond.).* 293:620–625.

Gething, M.-J., K. McCammon, and J. Sambrook. 1986. Expression of wild-type and mutant forms of influenza hemagglutinin: the role of folding in intracellular transport. *Cell.* 46:939–950.

Grasberger, B., A. P. Minton, C. DeLisi, and H. Metzger. 1986. Interaction between proteins localized in membranes. *Proc. Natl. Acad. Sci. USA.* 83:6258–6262.

Horwitz, M. S., M. D. Scharff, and J. V. Maizel. 1969. Synthesis and assembly of adenovirus 2. I. Polypeptide synthesis, assembly of capsomers, and morphogenesis of the virion. *Virology.* 39:682–694.

Hurtley, S. M., and A. Helenius. 1989. Protein oligomerization in the endoplasmic reticulum. *Annu. Rev. Cell Biol.* 5:277–307.

Hurtley, S. M., D. G. Bole, H. Hoover-Litty, A. Helenius, and C. S. Copeland. 1989. Interactions of misfolded influenza hemagglutinin with binding protein (BiP). *J. Cell Biol.* 108:2117–2126.

Jaenicke, R. 1987. Folding and association of proteins. *Prog. Biophys. Molec. Biol.* 49:117–237.

Klausner, R. D. 1989. Architectural editing: determining the fate of newly synthesized membrane proteins. *The New Biologist.* 1:3–8.

Knopf, P. M., and H. Lamfrom. 1965. Changes in the ribosome distribution during incubation of rabbit reticulocytes in vitro. *Biochim. Biophys. Acta.* 95:398–407.

Laemmli, U. K. 1970. Cleavage of structural proteins during the assembly of the head of bacteriophage T4. *Nature (Lond.).* 227:680–685.

Lazarovits, J., S.-P. Shia, N. Ktistakis, M.-S. Lee, C. Bird, and M. G. Roth. 1990. The effects of foreign transmembrane domains on the biosynthesis of the influenza virus hemagglutinin. *J. Biol. Chem.* 265:4760–4767.

Lodish, H. F. 1988. Transport of secretory and membrane glycoproteins from the rough endoplasmic reticulum to Golgi. *J. Biol. Chem.* 263:2107–2110.

Lodish, H. F., N. Kong, M. Snider, and G. A. M. Strous. 1983. Hepatoma secretory proteins migrate from the endoplasmic reticulum to Golgi at characteristic rates. *Nature (Lond.).* 304:80–83.

Machamer, C. E., R. W. Doms, G. B. Bole, A. Helenius, and J. K. Rose. 1989. Heavy chain binding protein recognizes incompletely disulfide-bonded forms of vesicular stomatitis virus G protein. *J. Biol. Chem.* 265:6879–6883.

Matlin, K. S., and K. Simons. 1983. Reduced temperature prevents transfer of a membrane glycoprotein to the cell surface but does not prevent terminal glycosylation. *Cell.* 34:233–243.

Matter, K., and H.-P. Hauri. 1991. Intracellular transport and conformational maturation of intestinal brush border hydrolases. *Biochemistry.* 30:1916–1923.

Ng, D. T. W., R. E. Randall, and R. A. Lamb. 1989. Intracellular maturation and transport of the SV5 type II glycoprotein HN: specific and transient association with GRP78-BiP in the ER and extensive internalization from the cell surface. *J. Cell Biol.* 109:3273–3289.

Pelham, H. R. B. 1989. Control of protein exit from the endoplasmic reticulum. *Annu. Rev. Cell Biol.* 5:1–23.

Peters, T., and L. K. Davidson. 1982. The biosynthesis of rat serum albumin. In vivo studies on the formation of the disulfide bonds. *J. Biol. Chem.* 257:8847–8853.

Pfeffer, S. R., and J. E. Rothman. 1987. Biosynthetic protein transport and sorting by the endoplasmic reticulum and the Golgi. *Annu. Rev. Biochem.* 56:829–852.

Randall, L. L., and S. J. S. Hardy. 1989. Unity in function in the absence of consensus in sequence: role of leader peptides in export. *Science (Wash. DC).* 243:1156–1159.

Rose, J. K., and R. W. Doms. 1988. Regulation of protein export from the endoplasmic reticulum. *Annu. Rev. Cell Biol.* 4:257–288.

Rothman, J. E. 1989. Polypeptide chain binding proteins: catalysts of protein folding and related processes in cells. *Cell.* 59:591–601.

Saraste, J., and E. Kuismanen. 1984. Pre- and post-Golgi vacuoles operate in the transport of semliki forest virus glycoproteins to the cell surface. *Cell.* 38:535–549.

Selimova, L. M., V. M. Zaides, and V. M. Zhdanov. 1982. Disulphide bonding in influenza virus proteins as revealed by polyacrylamide gel electrophoresis. *J. Virol.* 44:450–457.

Vuust, J., and K. A. Piez. 1972. A kinetic study of collagen biosynthesis. *J. Biol. Chem.* 247:856–862.

Wiley, D. C., and J. J. Skehel. 1987. The structure and function of the hemagglutinin membrane glycoprotein of influenza virus. *Annu. Rev. Biochem.* 56:365–394.

Wilson, I. A., J. J. Skehel, and D. C. Wiley. 1981. Structure of the haemagglutinin membrane glycoprotein of influenza virus at 3 Å resolution. *Nature (Lond.).* 289:366–373.

Yewdell, J. W., A. Yellen, and T. Bächi. 1988. Monoclonal antibodies localize events in the folding, assembly, and intracellular transport of the Influenza hemagglutinin glycoprotein. *Cell.* 52:843–852.